QFT FOR THE DESIGN OF AN AIRCRAFT FLIGHT CONTROL

A. Santander
RBIB/SAL, Robert Bosch España S.A., Madrid, Spain

J. Aranda
Dept. de Informática y Automática, E.S.I. Informática, UNED, Madrid, Spain

Abstract: Aircraft flight control has a multivariable and non linear nature that makes it suitable for a verification of control capability of different designs. QFT techniques have been thoroughly used during the last years to provide robust control designs while using classic theory of control. The QFT method is applied to the design of an aircraft flight control and the results, evaluated by means of an automated software, can be compared to results obtained with different methodology approaches.

Keywords: Control, Aircraft, MIMO, Nonlinear, Robust.

1. INTRODUCTION

QFT was first developed by Isaac Horowitz, (Horowitz 1982) and publications with QFT control techniques for flight control can be found in (Philips et al, 1997), (Lee et al, 2000), (Keating, et al, 1997), (Patcher et al, 1997), (Rasmussen S.J., Houpis C.H., 1997) and (Lin C, Ying C., 1998). In this paper, a QFT controller will be designed for the complete Research Civil Aircraft Model (RCAM) benchmark problem described by (Lambrechts, et al, 1997), which is a multivariable nonlinear plant that has been used to compare different design approaches. The results are analysed for both linear and nonlinear plants, by ways of an automated software. The designed controller results for both lateral and longitudinal dynamics can be compared to results from different robust approaches published in GARTEUR Action Group FM(AG08) (Magni et al, 1997)

2. PROBLEM DESCRIPTION

The problem corresponds to the RCAM design problem proposed for the GARTEUR Action Group FM(AG08). The non-linear model is used to generate linear plants that have been parametrized in order to get a quantitative model that is likely to be approached with QFT. The full model can be found in (Looye and Bennani, 1997). In this paper, we will centre the discussion on the lateral dynamic and the design of lateral controller is described. The longitudinal controller is obtained in a similar way.

The lateral model has eight possible measured outputs, Sideslip angle, Roll rate, Yaw rate, Roll angle, x component of inertial velocity in Fv, y component of inertial velocity in Fv, y position of aircraft in Fe and the inertial track angle, and 2 inputs, aileron deflection and rudder deflection. To simplify the design, a 2x2 MIMO system will be used composed of the two inputs, and the Sideslip angle, β, and Roll angle, ϕ, as outputs.
The longitudinal channel has seven possible inputs, pitch rate, q, horizontal load factor, nx, vertical load factor, nz, vertical velocity, w_V, z position, z, airspeed V_A, and total speed V, and two inputs, the throttles and the tail. The controller will use q and VA as outputs, and the two inputs.

The design specifications given by (Lambrechts, et al, 1997) are summarised as follows:

- Performance criteria:
  - Lateral deviation to be reduced to 10% in 30s.
  - Lateral commands to have Mp<5%.
  - Heading angle command with tr<10s, ts<30s and Mp<5%.
  - Altitude commands with tr <12s and ts <45s.
  - Step commands in altitude with Mp<5%.
  - Flight path angle with tr<5s and ts<20s.
  - Airspeed response with tr<12s and ts <45s.

- Robustness criteria: design should be able to cope with variations in the CoG, mass and speed.

3. CONTROLLER STRUCTURE

The controller has been designed in two stages, an inner loop, to augment system stability, and an outer loop for guidance control. The structure can be seen in Figure 1 and is valid for both lateral and longitudinal controller.

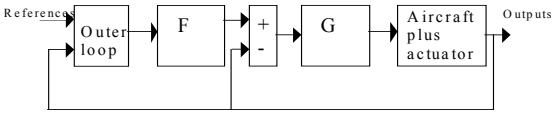

Figure 1. Structure of controller.

The inner loop for the lateral channel will have feedback from the two chosen variables, β and ϕ. The reference for the variable β will be the null value, and the ϕ variable will have as reference the outer loop, and will be used for tracking purposes. The longitudinal controller inner loop will use pitch rate, q, and airspeed, V_A as controlled variables and the outer loop will use the height as reference for pitch rate inner loop. The multivariable model will thus be reduced to two 2x2 MIMO problems.

4. CONTROLLER DESIGN

A detail explanation on lateral controller design is

$$A = \frac{.85^2}{s^2 + (2*.85)s + .85^2} \quad (1)$$

$$B = \frac{1}{s^2 + 2s + 1} \quad (2)$$

developed. In order to cope with design specifications, the optimal performance for β and ϕ is defined between the following two limiting functions:

In order to eliminate interaction between the two controlled variables, the controller will be designed to eliminate the coupling and the ideal behaviour can be seen with the lower and upper limits for tracking A_{cc} and B_{cc}. The chosen frequencies for the design are ω=[.1, .5, 1, 2] and the tracking specifications are in Table 1.

Table 1 Tracking specification for lateral inner loop

ω (rad/s)	A_β, A_ϕ	B_β, B_ϕ	A_{cc}	B_{cc}
.1	.98	.99	0	.25
.5	.74	.8	0	.38
1	.42	.5	0	.25
2	.15	.3	0	.25

The MIMO controller structure is chosen as a diagonal controller and diagonal prefilter. The ailerons will be controlled with the variable ϕ and the rudder will be controlled with the variable β. The design process will divide the problem into two sequential MISO problems (Yaniv, 1999). The set of plants {P} considered during the design have variations in Speed from 60 m/s to 90 m/s, CoG with variation in x axis from 0.15c to 0.31c, z axis of 0.0c to 0.15c, with c the mean aerodynamic chord, and mass, from 100.000 kg to 150.000 kg.

The MISO problem for the variable ϕ will be solved first. The low frequency bounds at ω=.1, .5, 1, 2 need to satisfy the following inequalities:

$$A_\phi \le \left| \frac{|g_{11} f_1| \pm |\pi_{12}| B_{cc}}{\pi_{11} + g_1} \right| \le B_\phi \; \forall P \in \{P\} \quad (3)$$

$$A_{cc} \le \left| \frac{\pi_{12} B_\beta}{\pi_{11} + g_1} \right| \le B_{cc} \; \forall P \in \{P\} \quad (4)$$

Where the notation $P^{-1} = [\pi_{ij}]$ has been used, being P the collection of plants. For robust stability, the following inequality should be satisfied for all frequencies:

$$\left| 1 + \frac{g_1}{\pi_{11}} \right| \ge 1.2 \forall P \in \{P\} \quad (5)$$

The bounds can be seen in the Figure 2, along with the nominal case with the controller g_1 calculated:

$$g_1 = \frac{-.766\left(\frac{s}{.2}+1\right)\left(\frac{s}{.5}+1\right)\left(\frac{s}{5.93}\right)}{s\left(\frac{s}{17}+1\right)} \quad (6)$$

In Figure 3 can be seen the prefilter that satisfies inequality (3):

$$f_1 = \frac{1}{\left(\frac{s}{.92}+1\right)\left(\frac{s}{1.34}+1\right)\left(\frac{s}{2.2}+1\right)\left(\frac{s}{10}+1\right)} \quad (7)$$

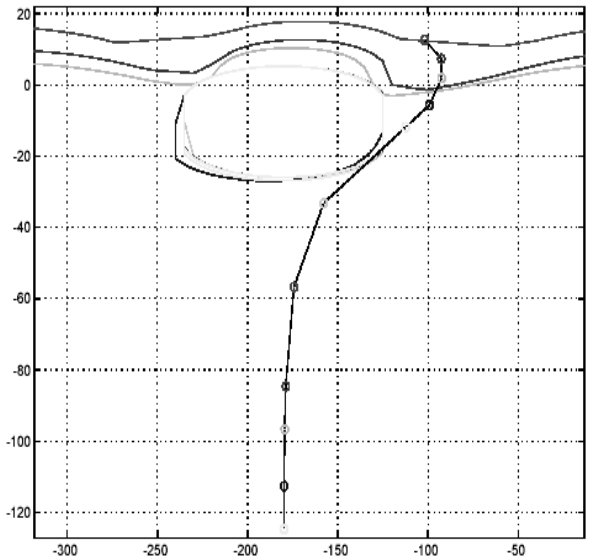

Figure 2. Nichols plot with bounds and nominal function with controller for ϕ.

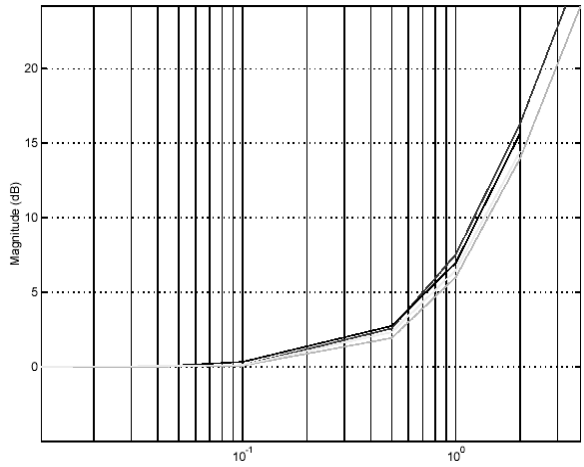

Figure 3. Resulting Bode with prefilter applied.

The results for the ϕ controller are used in the design of the controller for β. The controller g_2 and prefilter f_2 for the MISO problem need to satisfy the following inequalities:

$$A_{cc}(\omega) \le \left| \frac{\pi_{21}^2 f_1}{\pi_{22}^2 + g_2} \right| \le B_{cc}(\omega); \forall P \in \{P\} (8)$$

$$A_{\beta}(\omega) \le \left| \frac{g_2 f_2}{\pi_{22}^2 + g_2} \right| \le B_{\beta}(\omega); \forall P \in \{P\} (9)$$

Where

$$\pi_{21}^2 = \frac{\pi_{21} g_1}{\pi_{11} + g_1} (10)$$

$$\pi_{22}^2 = \pi_{22} - \frac{\pi_{21}\pi_{12}}{\pi_{11} + g_1} (11)$$

As with the ϕ case, robust stability is defined by the following inequality that must be fulfilled at all frequencies.

$$\left| 1 + \frac{g_2}{\pi_{22}^2} \right| \ge 1.2 \forall P \in \{P\} (12)$$

The calculated bounds for inequalities and the nominal loop with the controller are shown in Figure 4. The controller g_2 calculated is:

$$g_2 = \frac{2.981\left(\frac{s}{.75}+1\right)\left(\frac{s}{1.23}+1\right)\left(\frac{s}{3.46}+1\right)}{s\left(\frac{s}{5}+1\right)} (13)$$

The calculated prefilter is:

$$f_2 = \frac{1}{\left(\frac{s}{0.4}+1\right)\left(\frac{s}{0.9}+1\right)\left(\frac{s}{2.3}+1\right)} (14)$$

An outer loop controller is added for tracking purposes. The lateral deviation is used as a reference value for the ϕ variable. The resulting outer controller is:

$$g_\phi = 0.015s \quad (15)$$

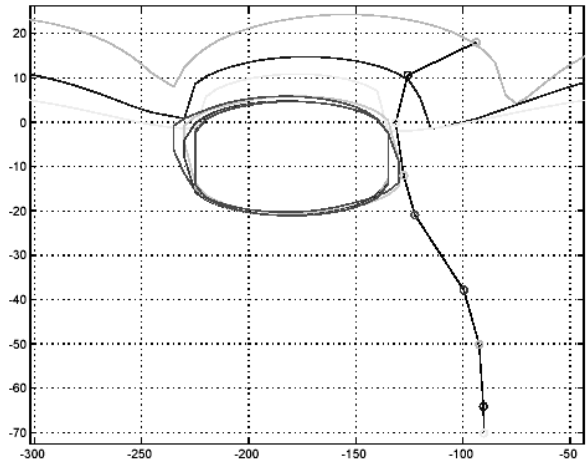

Figure 4. Nichols plot with bounds and nominal loop with controller for β.

Due to the excess of zeros over poles in (6) and (13), a pole far from origin is added in both of them to perform the simulations. Figure 5 shows the response of sixteen linearised systems to a step in lateral commands. The rise time and settling time comply with specifications while the control effort is minimised.

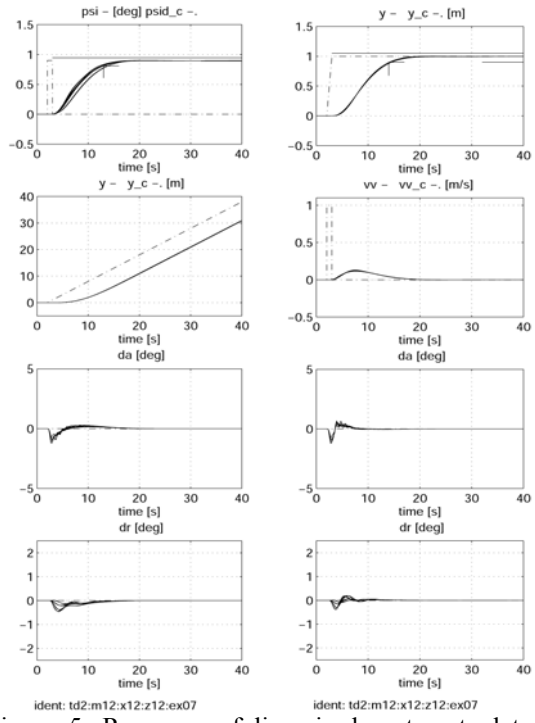

Figure 5. Response of linearised system to lateral commands.

An analysis of the inner loop shows that the specifications are fulfilled. The Phi and Beta channels behave as (1) and (2) and the cross coupling has been reduced according to table 1 specifications. The results for 60 plants can be seen in Figure 6.

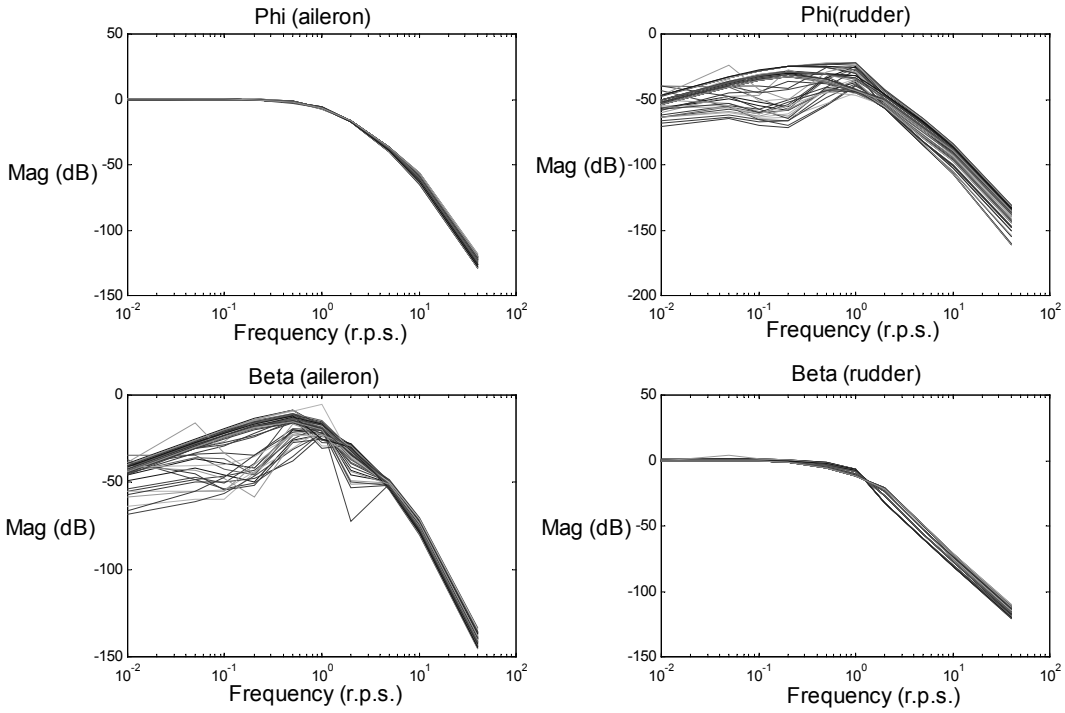

Figure 6. Lateral inner loop controller analysis.

The longitudinal controller is designed in a similar way. The measured variables chosen are the pitch rate, q, and the airspeed, V_A. An inner loop controller is designed for stability augmentation and an outer loop controller will be used to obtain a reference for the q variable inner loop. The controller for q inner loop is:

$$g_3 = \frac{-11.89\left(\frac{s}{0.6}+1\right)\left(\frac{s}{2.5}+1\right)\left(\frac{s}{9}+1\right)}{s\left(\frac{s}{0.289}+1\right)} \quad (16)$$

And the prefilter f_3:

$$f_3 = \frac{1}{\left(\frac{s}{0.0962}+1\right)\left(\frac{s}{0.319}+1\right)} \quad (17)$$

The inner loop for V_A has the controller:

$$g_4 = \frac{0.1\left(\frac{s}{0.73}+1\right)}{\left(\frac{s}{5.4}+1\right)} \quad (18)$$

In the case of airspeed, no prefilter is used. The outer loop for the longitudinal controller is found to be as follows:

$$g_q = -0.003s(s+1.66) \quad (19)$$

For the implementation of (16), a pole far from the origin is added due to the excess of zeros over poles. The response of the linearised system to an step in altitude can be found for sixteen extreme cases in Figure 7. Rise time and settling time are within specifications. Only flight path angle shows a rise time a little bit above the required rise time.

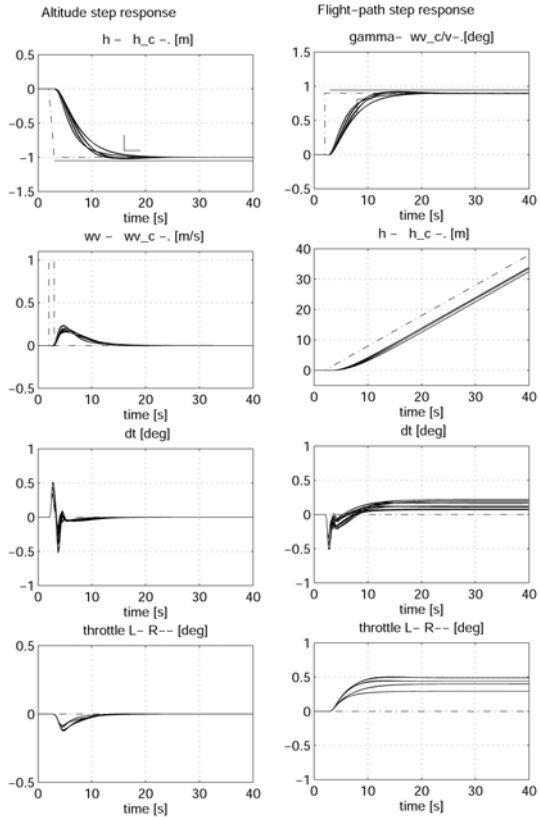

Figure 7. Step responses to longitudinal commands of linearised systems.

The response of the air speed can be seen in Figure 8, in which can also be seen the effect of windshear. The specifications are fulfilled also, with a rise time faster than specified.

Both lateral and longitudinal channels show appropriate responses in the linarised system. The

non linear behaviour will be discussed in the next section, along with the robustness of the system to changes in the CoG.

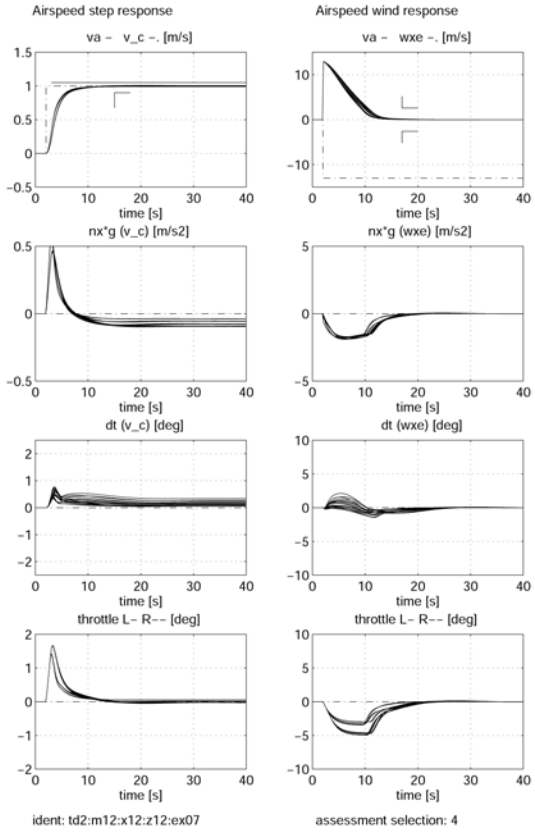

Figure 8. Step responses of Airspeed and response to windshear.

5. NON-LINEAR SIMULATION RESULTS

This section is based in the evaluation mission in (Lambrechts, et al, 1997). Three different configurations for CoG are simulated in a landing trajectory. A fourth case considers a time delay of 100ms. The trajectory is divided in four segments, each one of them testing different features for the aircraft.

Figure 9 plots the trajectory followed during the landing configuration by the controlled aircraft, as well as the tracking reference. The four segment limits are identified by numbers.

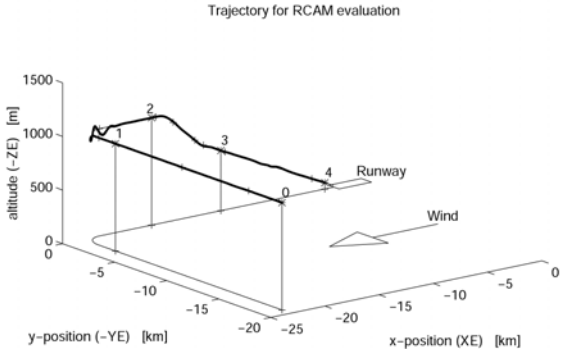

Figure 9. Trajectory followed by the model.

Figure 10 shows the performance in the first segment (from 0 to 1). During this segment, the failure of one of the engines is simulated. The failure occurs at point a and ends at point b. It is clearly seen that the aircraft deviation from ideal performance is at some points close to the allowed 20m deviation, but fulfils with design specifications.

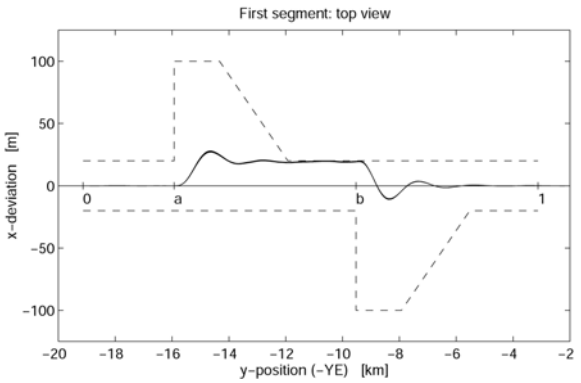

Figure 10. The effect of engine failure.

Figure 11 shows the performance of the controller during a 90 degree turn (from point 1 to point 2). The turn does not follow the ideal performance during part of the time but mostly complies with the limits imposed. The 90 degree turn rate is difficult to achieve and the acceleration needed to follow the ideal performance will be over the design limits. This will be seen in the numerical results with comfort factor over the design limit.

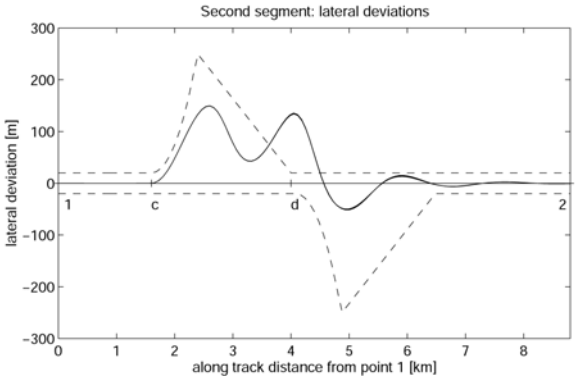

Figure 11. Lateral deviation during 90 degree turn.

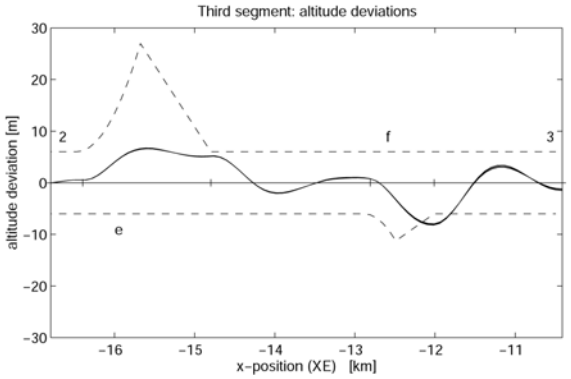

Figure 12. Altitude deviations during altitude change segment.

Figure 12 shows the altitude change phase (from point 2 to point 3). The performance is good during all the phase. As with the 90 degree turn, the acceleration needed to cope with the altitude change will demand a vertical acceleration over the comfort limits, that will reduce the comfort performance during this segment.

Figure 13 shows the performance during the final approach (from point 3 to point 4).The controller is capable of maintaining the aircraft inside the limits imposed by the performance specification.

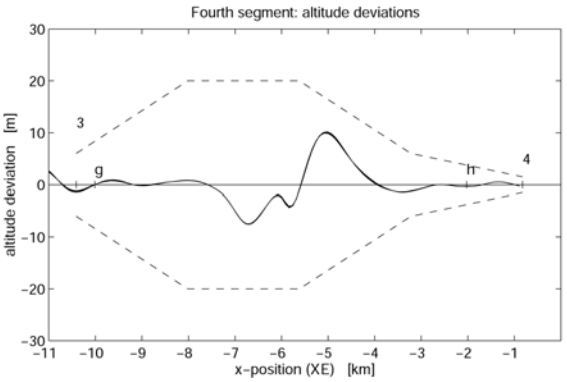

Figure 13. Vertical deviations during final approach.

Table 2 shows a summary of the performance achieved during each of the segments. The design objective is to keep the numerical results below unity, which would mean a limiting compliance with performance specification. The values obtained are below unity except for comfort factor in the second and third segments. The comfort values over unity are due to the acceleration needed to cope with the 90 degree turn during the second segment and the change in altitude during the third segment, which are over the design specification requirements. Total average value is within limits. The performance factor shows good compliance with ideal performance. The performance deviation factor is taken as a measurement of the robustness of the design to parameter variation. The value obtained well below unity shows good robustness of the design. The safety factor is a measure of the stability of the design. The values obtained for all the segments are below unity. The power factor is a measure of the usage of the actuators. All values are below unity, which indicates the controller maintains the actuators far from saturation limits.

Table 2 Numerical results of the evaluation procedure.

	Segment I	Segment II	Segment III	Segment IV	Total
Performance	0.1404	0.3928	0.2564	0.3359	0.2814
Perf. Dev.	0.0274	0.0467	0.1820	0.1243	0.0951
Comfort	0.3668	1.6085	1.4657	0.5435	0.9961
Safety	0.0042	0.3068	0.0084	0.1085	0.1070
Power	0.0025	0.0104	0.0148	0.0302	0.0145

6. CONCLUSIONS

QFT design technique has been used for a multivariable control design problem. The results are comparable to results obtained with different approaches used to solve the same design problem. The economy of the design, with a reduction of the controlled variables to four, two in the lateral controller and two in the longitudinal controller, makes QFT approach useful to reduce complex problems to simpler ones. The QFT method is appropriate for robust design and is specially useful when some parameter uncertainty appears in the plant to be controlled. The design obtained for the linearised plant has been sufficient to fulfil design requirements in the non linear plant, with numerical results within the limits imposed for the problem.

ACKNOWEDGEMENTS

Part of this development was supported by MCyT of Spain under contract DPI2003-09745-C04-01.

REFERENCES

Bennani, S, Looye, G, 1997. *Description and analysis of the Research Civil Aircraft Model (RCAM)*. Technical Publication TP-088-27, Group for Aeronautical Research and technology in Europe GARTEUR-FM(AG08)

Horowitz I., 1992.*Quantitative Feedback Design Theory – QFT*. QFT Publications.

Keating M.S., Patcher M., Houpis C.H., 1997. *Fault tolerant flight control system: QFT design*. International journal of robust and nonlinear control. VOL 7, 551-559.

Lambrechts, P, Bennani, S, Looye, G, Helmersson, A 1997. *Robust flight control design challenge problem formulation and manual: the research civil aircraft model (RCAM)*. Technical Publication TP-088-3, Group for Aeronautical Research and technology in Europe GARTEUR-FM(AG08)

Lee, J.W., Chait, Y, Steinbuch, M, 2000. *On QFT tunning of multivariable μ controllers*. Automatica 36 (2000) 1701-1708.

Lin C., Ying C., 1998. *Design and aplication of multivariable robust optimal systems*. Optimal Control Aplication & Methods, 19, 23-39.

Magni J.F, Bennani S., Terlouw J., 1997. *Robust Flight Control. A design challenge*. Springer.

Patcher M., Houpis C.H., Trosen W., 1997. *Design of an air-to-air automatic refueling flight control system using quantitative feedback theory*. International journal of robust and nonlinear control, VOL 7, 561-580.

Philips S.N., Patcher M, Houpis C.H., Rasmussen S.J., 1997. *A QFT subsonic envelope flight control system design*. International Journal of Robust and Nonlinear Control, Vol 7, 581-589.

Rasmussen J. Houpis C.H., 1997. *Development, implementation and flight test of a MIMO digital flight control system for an unmanned research vehicle designed using quantitative feedback theory. International journal of robust and nonlinear control*. Vol 7, 629-642.

Yaniv, O, 1999. *Quantitative feedback design of linear and nonlinear control systems*. Kluwer Academic Publishers.